Full-dimensional (15-dimensional) ab initio analytical potential energy surface for the H7+ cluster

Patricia Barragán, Rita Prosmiti, Yimin Wang, and Joel M. Bowman

Citation: J. Chem. Phys. **136**, 224302 (2012); doi: 10.1063/1.4726126
View online: http://dx.doi.org/10.1063/1.4726126
View Table of Contents: http://jcp.aip.org/resource/1/JCPSA6/v136/i22
Published by the American Institute of Physics.

Full-dimensional (15-dimensional) *ab initio* analytical potential energy surface for the H_7^+ cluster

Patricia Barragán,[1,a)] Rita Prosmiti,[1,b)] Yimin Wang,[2] and Joel M. Bowman[2,c)]
[1]*Instituto de Física Fundamental, CSIC, (IFF-CSIC), Serrano 123, 28006 Madrid, Spain*
[2]*Department of Chemistry and Cherry L. Emerson for Scientific Computation, Emory University, 1515 Dickey Drive, Atlanta, Georgia 30322, USA*

(Received 28 March 2012; accepted 21 May 2012; published online 11 June 2012)

Full-dimensional *ab initio* potential energy surface is constructed for the H_7^+ cluster. The surface is a fit to roughly 160 000 interaction energies obtained with second-order MöllerPlesset perturbation theory and the cc-pVQZ basis set, using the invariant polynomial method [B. J. Braams and J. M. Bowman, Int. Rev. Phys. Chem. **28**, 577 (2009)]. We employ permutationally invariant basis functions in Morse-type variables for all the internuclear distances to incorporate permutational symmetry with respect to interchange of H atoms into the representation of the surface. We describe how different configurations are selected in order to create the database of the interaction energies for the linear least squares fitting procedure. The root-mean-square error of the fit is 170 cm^{-1} for the entire data set. The surface dissociates correctly to the $H_5^+ + H_2$ fragments. A detailed analysis of its topology, as well as comparison with additional *ab initio* calculations, including harmonic frequencies, verify the quality and accuracy of the parameterized potential. This is the first attempt to present an analytical representation of the 15-dimensional surface of the H_7^+ cluster for carrying out dynamics studies. © *2012 American Institute of Physics*. [http://dx.doi.org/10.1063/1.4726126]

I. INTRODUCTION

The protonated hydrogen clusters, $H_3^+(H_2)_n$, with $n \geq 1$, and their deuterated isotopic species, are of fundamental interest in a series of phenomena involving Coulomb explosions, as well as through reactions of astrophysical interest to nuclear fusion reactions producing high energy neutrons, and also as a possible medium for energy storage (see Refs. 1–4 and references therein). A number of experimental and theoretical studies have suggested a shell model structure for these clusters with an H_3^+ core surrounding by several H_2 molecules. The support of this model is based on experimental data from mass spectra, infrared predissociation spectra, and dissociation enthalpies.[5–11] Theoretically, apart from the numerous electronic structure calculations on the equilibrium structures of these systems (see, e.g, Refs. 12–15), more recently, several dynamics studies have been reported in the literature for the H_5^+.[16–26] For larger clusters of this series such investigations are still limited to the earlier work by Štich *et al.*[27] based on *ab initio* path integral molecular dynamics simulations for the H_5^+, H_7^+, H_9^+, and H_{27}^+ clusters, showing, for first time, the high fluxional nature of these systems.

Unfortunately, still no model potential is available for larger H_n^+, with $n = 7, 9, \ldots$, clusters, which would allow dynamics calculations similar to those for the H_5^+. The representation of a potential energy surface (PES) is getting complicated and laborious task, as the number of atoms increases. Thus, the complexity of the processes to be studied compromises the description of the PES, e.g., local or global, with a global, full-dimensional and high-level *ab initio*-based PES to be the ideal choice. However, for complexes with more than four atoms the overall cost for the traditional analytical fitting or interpolation procedures could be often relatively high, and then direct/"on the fly" calculation of the potential could be a competitive approach to be employed.[22,27,28] Just recently, a DFT-based "on the fly" PES has been reported for the H_7^+,[29] using the B3(H) functional, specifically designed for hydrogen-only systems.[30] It has been shown that such functional parameterization based on molecular properties, instead on atomic ones,[29–31] could provide a realistic and quite accurate description of the cluster surface at relatively low computational cost. Although, we should note that in general an analytical representation is much more efficient computationally, and also higher level of *ab initio* theory could be used. Motivated by this, we focus our interest here on the generation of an analytical full-dimensional potential surface of the H_7^+ cluster. Even beyond the challenge of the high dimensionality, we should further count with a large degree of floppiness for this system.

Following the traditional way to represent a PES in this field, so far various strategies to deal with high-dimensional potentials have been developed.[16,32–36] The H_7^+ has 15 degrees of freedom, contains 7 identical H (light) atoms, and thus its PES representation should be invariant with respect to all permutations. For that, we have implemented the approach proposed by Braams and Bowman,[36] that is based on global fitting of *ab initio* electronic energies by incorporating permutational symmetry directly into the representation of the PES, using fitting basis functions that are invariant with respect to all permutations of identical atoms. In this way, the invariance

a)Present address: CELIA, Université de Bordeaux-I, UMR CNRS 5107, CEA, 351 Cours de la Libération, F-33045 Talence, France.
b)E-mail: rita@iff.csic.es.
c)E-mail: jmbowma@emory.edu.

property of the PES leads to a reduction of the configurations to be sampled, and thus to the number of *ab initio* energies to be computed. This approach has been applied to generate the potential energy surfaces of more then 20 molecular systems (see Refs. 17, 37–39).

In this paper, we present a first attempt for an analytical representation of the 15-dimensional surface of the H_7^+ cluster. The surface we describe is constructed from nearly 160 000 *ab initio* MöllerPlesset perturbation theory (MP2) energies. Section II discusses the details of such calculations and fitting procedure used. In Sec. III we present the properties of the PES together with the tests of accuracy of it in representing the *ab initio* data, structure, and energetics of various stationary points, asymptotic behavior, and dissociation features. Finally, a summary and some conclusions are given in Sec. IV.

II. METHODS AND CALCULATION DETAILS

A. *Ab initio* calculations and grid generation procedure

Up to date only electronic structure calculations on the equilibrium structure of H_7^+ are available in the literature.[12–15] Thus, we list in Table I some results of the present calculations on the optimized energy and structure at MP2 and coupled-cluster single double (triple) (CCSD(T)) levels of theory, and compare them with the best known values in the literature.[15] All *ab initio* calculations are carried out using the MOLPRO 2009 (Ref. 40) package. We performed various test calculations employing different basis sets, however, we only present here the ones with the cc-pVQZ and cc-pV5Z basis, as they are found to be computationally more efficient. In Figure 1 we display the CCSD(T)/cc-pVQZ optimized structure of H_7^+, that is of C_{2v} symmetry in accord with all present and previous calculations. In all our calculations the Cartesian coordinates are used, although in order to facilitate the presentation of the H_7^+ cluster here, we introduce the R_1,R_2, and R_3 for the HH bondlengths of the H_3^+ core, P_1 and P_2 for the H_2 distances, while D_1 and D_2 are the intermolecular distances as they described in Figure 1. One can see in Table I the effect of the method and the basis set on the total energies of the optimal structures for both H_7^+, E_{opt}, and $H_5^+ + H_2$ fragments, $E_{diss} = E_{opt}^{H_5^+} + E_{opt}^{H_2}$, as well as on the equilibrium configuration of H_7^+. In particular, the MP2 results predict a more compact geometry for the H_3^+ and H_2 moieties, and somehow more elongated $D_{1,2}$ distances than the CCSD(T) ones. This is reflected in the total energy values, and to the well-depths with respect to $H_5^+ + H_2$ limit. One can see that for the D_e differences of 20 cm^{-1} are obtained between MP2 and CCSD(T) results using the same basis set, while differences in the range of 25–65 cm^{-1} are found compared all of them to the CCSD(T)/common board sets (CBS) value.

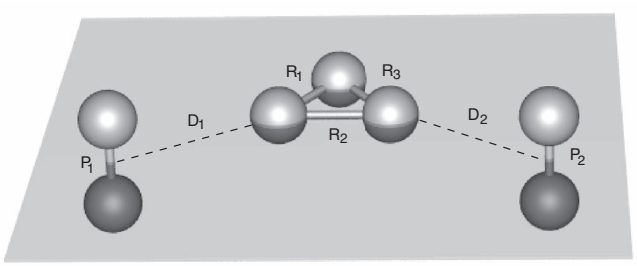

FIG. 1. Optimal structure of the H_7^+ from the CCSD(T)/cc-pVQZ calculations, and schematic description of the internal coordinates used.

As we mentioned above, the H_7^+ is a floppy molecule, and our *ab initio* data should sample a broad regions of the configuration space, covering both equilibrium geometries and the dissociation to $H_5^+ + H_2$ region. Therefore, for the grid generation of the present database of configurations we combined different strategies. The majority of the configurations are obtained by performing direct/"on the fly" Monte Carlo simulations according to Boltzmann statistics sampling broad energy regimes at the MP2/cc-pVQZ level. In this way 58 180 configurations are calculated covering energies up to −3.68038 a.u., and 95 000 configurations for energies up to −3.42276 a.u., while 2346 configurations are generated for various orientations of the $H_5^+ + H_2$ by varying their intermolecular distance in order to describe their dissociation limit up to energies of 3.6694855 a.u. Moreover, in order to include specific conformations of the H_3^+ and H_2 subunits an additional set of 4425 energies were computed by varying the R_1, R_3 and P_1, P_2, respectively, as a function of D_2 and $D_1 = D_2$ distances up to an energy of −3.32769946 a.u.

The energy distribution of the MP2 *ab initio* data used in the fitting procedure is shown in Figure 2. One can see that a large number of points is accumulated at the low energy regime up to 2000 cm^{-1} above the potential minimum, and up to energy of 27 000 cm^{-1} we have almost the entire set of data.

B. Fitting the potential energy surface

The H_7^+ is an 7-atom system and 15 degrees of freedom are needed to describe its potential energy surface, that is invariant with respect to all permutations of the seven H

TABLE I. Total energies (in a.u.), and bond lengths (in Å) of the optimal H_7^+ structure obtained by the indicated method/basis calculations. Total energies (in a.u.) for the $H_5^+ + H_2$ dissociation, and well-depth value (in cm^{-1}) with respect to this limit at each level of calculation are also given.

Method/basis set	E_{opt}	$R_{1,3}/R_2$	$D_{1,2}$	$P_{1,2}$	E_{diss}	D_e
MP2/cc-pVQZ	−3.69009130	0.86721/0.93490	1.58009	0.74903	−3.68222854	1725.7
MP2/cc-pV5Z	−3.69219685	0.86695/0.93400	1.58153	0.74879	−3.68424649	1744.9
CCSD(T)/cc-pVQZ	−3.71237896	0.87171/0.94148	1.57266	0.75474	−3.70571378	1744.6
CCSD(T)/cc-pV5Z	−3.71375501	0.87144/0.94082	1.57344	0.75449	−3.70442994	1764.9
CCSD(T)/CBS Ref. 15	−3.71453	0.87211/0.94115	1.57382	0.75496	−3.70637	1790.9

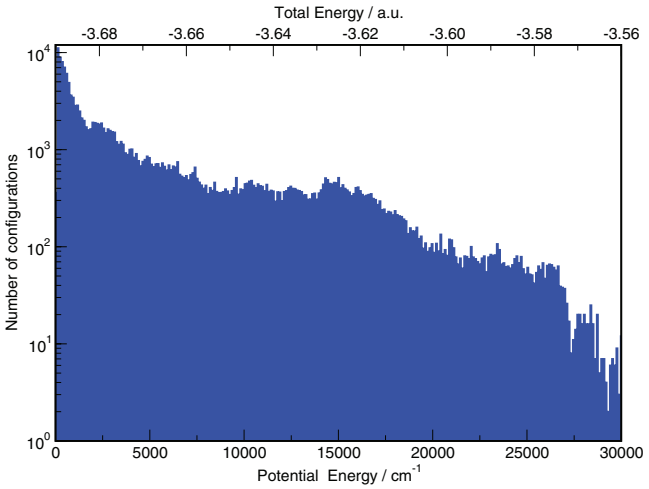

FIG. 2. Distribution of total and relative, with respect to the optimal value, MP2 electronic energies used for the fitting of the H_7^+ surface.

atoms, i.e., 7! = 5040. We employed the invariant polynomial method,[36] and we used a single expression to represent the potential energy function containing the seven-body term given as follows:

$$V(\mathbf{y}) = \sum_{\alpha=1}^{M} h_\alpha(\mathbf{p}(\mathbf{y}))q_\alpha(\mathbf{y}), \quad (1)$$

where $\mathbf{p}(\mathbf{y})$ is the vector formed by 21 primary invariant polynomials, $q_\alpha(\mathbf{y})$ (for $1 \le \alpha \le M$) are the secondary invariant polynomials, and h_α is an arbitrary polynomial. The primary and secondary polynomials are functions of Morse-like functions, $y(i, j) = \exp(-r(i, j)/\lambda)$, where λ was fixed at 2.0 Bohr and $r(i, j)$ is the internuclear distance of atom i and j. We used the complete molecular symmetry group, of degree 7!(=5040), to define the space of invariant polynomials, and as in our earlier work the MAGMA computer algebra system[41,42] was employed to help generate the basis. All the coefficients of the potential representation term are fitted in a standard least-squares optimization, and a code for the generation of the PES is available upon request.

III. RESULTS AND DISCUSSION

A. Properties and topology of the PES

Fitting accuracy: In Table II we list the fitting error, root-mean-square (rms), between the MP2 data and the PES, using permutationally invariant polynomials of different total degree, e.g., up to 5, 6, and 7, with 95, 268, and 739 terms in the fit, respectively. As seen an overall rms of 170 cm^{-1} is achieved with M = 7. In Table III we present the rms error

TABLE II. Comparison of different order fits of the PES. M is the total degree of the invariant polynomials. The rms errors are given in cm^{-1}.

M	Coef. No.	rms/weighted rms
5	95	228/134
6	268	174/107
7	739	170/105

TABLE III. Number of configurations and their corresponding rms value (in cm^{-1}) at the indicated energy ranges. Energy limits in a.u.

Energy range/limit	Config. No.	rms
Below $H_5^+ + H_2$/−3.68222854	69 868	30.5
Below H_5^+ (ZPE) + H_2(ZPE)/−3.64431107	128 770	110.7
All H_7^+ energies/−3.32769946	159 951	170.2

of this fit with respect to different subset of *ab initio* energies. The error obtained over ∼70 000 configurations with energies below the $H_5^+ + H_2$ dissociation limit is about only 30 cm^{-1}, while is roughly four times larger, 111 cm^{-1}, for energies up to the sum of harmonic zero point energies (ZPE), at MP2/cc-pVQZ level, of the fragments. In Figure 3 we show a more detailed analysis of the rms error as a function of the MP2 energies, and the number of configurations every 5000 cm^{-1}, that demonstrates the quality of the fitted PES up to energies of 20 000 cm^{-1}.

Stationary point analysis: Based on MP2 and CCSD(T) calculations using the cc-pVQZ basis set we locate 10 stationary points of the H_7^+ cluster. The results of the optimized structures at MP2 level of theory are depicted in Figure 4, while their energetics are given in Table IV in comparison with the optimized CCSD(T) data, as well as with the values obtained with the fitted PES. The optimal configuration for H_7^+ is a C_{2v} symmetry structure with the two H_2 being perpendicular attached to a H_3^+ unit. As it can be seen the structures of the next stationary points are also highly related with those for the H_5^+ cluster.[43] In particular, the 2-C_s conformer lying 47 cm^{-1} above the global minimum, corresponds to a planar H_5^+ and a perpendicular H_2 unit. This is a first-order saddle point corresponding to a 90° rotation of one of the H_2 moieties, and with energy difference respect to the global minimum very similar to those of the corresponding H_5^+ structures. The next one is the planar 3-C_{2v} configuration at energy of 112 cm^{-1}, and is a second-order saddle point. These first three conformers are very close in energy, while the second group of structures consists of 4 geometries, namely, 4-C_{2v}, 5-C_{2v}, 6-C_{2v}, 7-C_{2v}, which are lying much higher in energy, and correspond to planar and/or non-planar combinations of

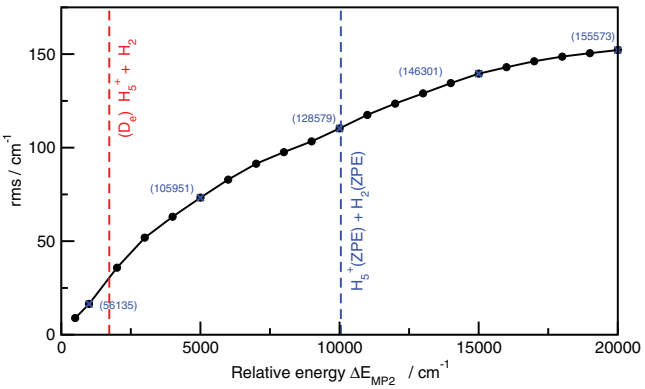

FIG. 3. Root-mean-square error (rms) of the H_7^+ PES as a function of relative MP2 energy values with respect to the global minimum one. The number of configurations below the energies of 1000, 5000, 10 000, 15 000, and 20 000 cm^{-1} are shown in parenthesis.

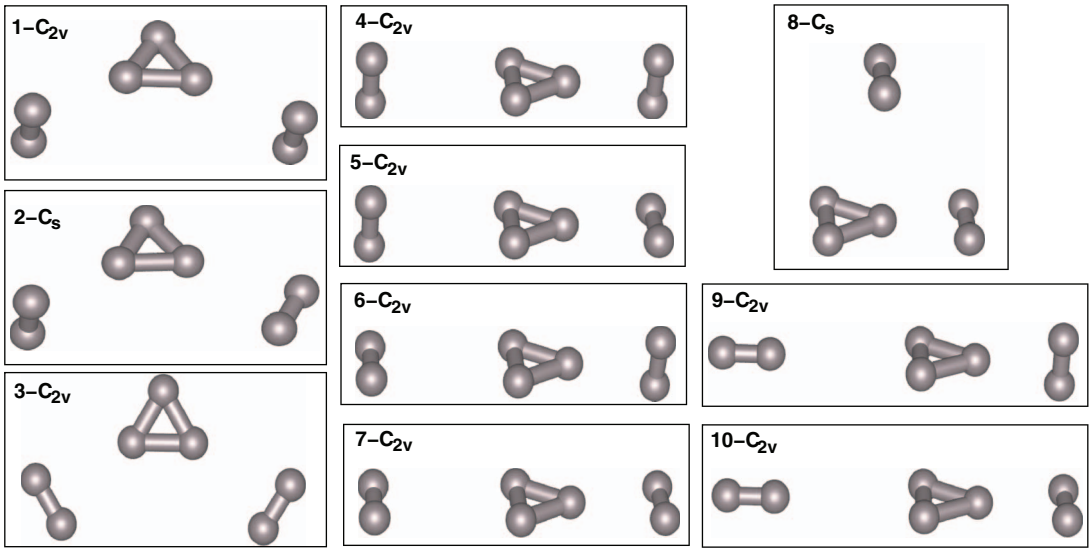

FIG. 4. Optimized structures of low-lying stationary points of H_7^+ at MP2/cc-pVQZ level of theory.

the two H_2, with each of them being attached to the opposite ends of an elongated H_3^+ core. The 4-C_{2v} is a first-order saddle point connecting the two equivalent 1-C_{2v} minima, while the rest ones are second- and third-order saddle points corresponding to in and out of plane rotations of one or two H_2 units. One can see that the barriers of such rotations are 71, 81, and 157 cm^{-1}, respectively, which are slightly higher than the ones for the H_2 rotations in the 1-C_{2v} global minimum. The next structure, 8-C_s, is lying at 1113.8 cm^{-1}, while the 9-C_{2v} and 10-C_{2v} ones are found to be at 1630.9 and 1717.5 cm^{-1}, respectively. We should mention here that the different groups of stationary points are clearly combinations of stationary points of the H_5^+, e.g., the 2nd group comes from the 5-1, 5-3, 7-1, and 7-3, the 8-C_s from the 9-1 and the 9-C_{2v}, and 10-C_{2v} from the 8-1, and 8-3 structures of the H_5^+, respectively. Also, we should point that for the H_7^+, apart from the three first, the present stationary points are probably not the lowest lying in energy ones, contrary to the H_5^+.[43]

A comparison of the energies of these stationary points obtained by the fitted PES and the MP2 *ab initio* data is presented in Table IV. The analytical surface predicts the same ordering of these points, except for the 5-C_{2v} and 6-C_{2v} conformers that are in a reverse order. The maximum deviation of the fitted PES values compared to the MP2 ones is found to be 73.3 cm^{-1} for the 8-C_s MP2 optimal structure, and the minimum deviation is 0.2 cm^{-1} for the global minimum MP2 configuration. When now we compare the potential values at the optimized configurations from the MP2 and the fitted PES (see values in parenthesis in Table IV) then these differences count to 41.8 and 0.09 cm^{-1} for the 8-C_s and 1-C_{2v}, respectively. As seen, a very good agreement is obtained, especially none of these stationary points are explicitly included in the data used for the fit. Further, we also compare the energies and structures of the stationary points of the MP2 calculation, with the results of CCSD(T) optimizations using the same basis set, and we consider them as the benchmark data (see Table IV). We show that the present MP2 energies, and thus

TABLE IV. Total energy (in a.u.) for the global minimum structure, and relative energies (in cm^{-1}) with respect to it for the indicated stationary points of H_7^+ at the CCSD(T) and MP2 levels of theory, together with the values of the current PES. The PES^{opt} values (in parenthesis) correspond to the potential energy at the optimized geometry of the fitted surface. The energy differences, E_{diff} in cm^{-1}, between the MP2 and the fitted PES values for the corresponding MP2 optimized and PES^{opt} (in parethesis) configurations are also listed. N indicates the order of the stationary point.

		Energy			
Config. No.	N	CCSD(T)	MP2	PES(PES^{opt})	E_{diff}
1-C_{2v}	0	−3.71237896	−3.69009130	−3.6900904(−3.6900909)	− 0.2(−0.09)
2-C_s	1	47.0	47.0	48.3(48.2)	1.3(1.2)
3-C_{2v}	2	112.0	112.2	115.4(114.7)	− 3.2(−2.5)
4-C_{2v}	1	847.8	831.7	843.6(842.2)	− 11.9(−10.5)
5-C_{2v}	2	921.2	903.2	934.1(932.2)	− 30.9(−29.0)
6-C_{2v}	2	927.7	912.7	905.5(904.5)	7.2(8.2)
7-C_{2v}	3	1006.2	989.2	1000.1(998.3)	− 10.9(−9.1)
8-C_s	2	1117.8	1113.8	1187.1(1155.6)	− 73.3(−41.8)
9-C_{2v}	3	1626.3	1630.9	1618.5(1611.6)	12.4(19.3)
10-C_{2v}	4	1715.5	1717.5	1736.6(1728.2)	− 19.1(−10.1)

TABLE V. Comparison of the harmonic frequencies of PES for the 1-C_{2v} minimum of the H_7^+ with the MP2 and CCSD(T) optimized calculations.The corresponding ZPE values are also listed.

	1-C_{2v}		
Mode	CCSD(T)	MP2	PES
1	97	106	99
2	124	129	125
3	170	170	170
4	408	406	432
5	564	556	563
6	577	583	603
7	697	705	699
8	737	738	759
9	801	813	840
10	915	920	936
11	2286	2345	2353
12	2527	2567	2580
13	3289	3338	3350
14	4238	4341	4296
15	4241	4344	4317
Harmonic ZPE	10 836	11 031	11 061

the PES based on them, agree very well with the benchmark CCSD(T) values. We found rather small differences, less than 18 cm^{-1}, between the relative CCSD(T) and MP2 energies for these stationary points, that is within the rms error value of 30.5 cm^{-1} for energies below the $H_5^+ + H_2$ dissociation at 1725.7 cm^{-1} (see Table III). By comparing now the energy values of the fitted surface with the CCSD(T) ones we obtained a maximum difference of 37.8 cm^{-1} for the 8-C_s stationary point, and an averaged absolute difference of only 12 cm^{-1} for all of them.

In turn, we consider the normal-mode frequencies associated with all these stationary points. The energy gradients are obtained numerically for the analytical PES. The harmonic vibrational frequencies for the global 1-C_{2v} minimum and the corresponding ZPE calculated from the PES are listed in Table V in comparison with the ones obtained from the CCSD(T) and MP2 calculations. One can see that the frequencies values predicted by the PES are in agreement with both *ab initio* computations, with similar deviations from them and the larger ones, about 70 cm^{-1}, are found for the H_2 frequencies. The results of the harmonic frequencies for the ten stationary points from the MP2 optimization calculations together with the ones predicted by the PES are given in the supplementary material.[44] The number of negative frequencies indicates the order of the saddle point, as it is given in Table IV. We found that the PES predicts exactly the same order for each saddle point as the CCSD(T) and MP2 calculations, and also the frequencies for each normal-mode are in accord with those obtained from the benchmark ones.

Asymptotic/ $H_5^+ + H_2$ dissociation behavior: The first dissociation limit for the H_7^+ corresponds to the lost of one H_2 molecule, e.g., $H_5^+ + H_2$. Thus, we performed a series of calculations considering various intermolecular distances between the two fragments, as well as several relative orientations of them. The H_5^+ and H_2 units are fixed at their equilibrium geometries at CCSD(T) level, and their intermolecular distance R, between the center of mass of the H_3^+ core to the center of mass of the dissociating H_2, is varied up to 15Å. The geometries of the 10 low-lying stationary points of the H_5^+ are chosen together with planar and non planar, with respect the H_3^+ core, orientations for the second H_2 molecule. In Figure 5 we present the potential curves obtained from the present PES in comparison with their corresponding MP2

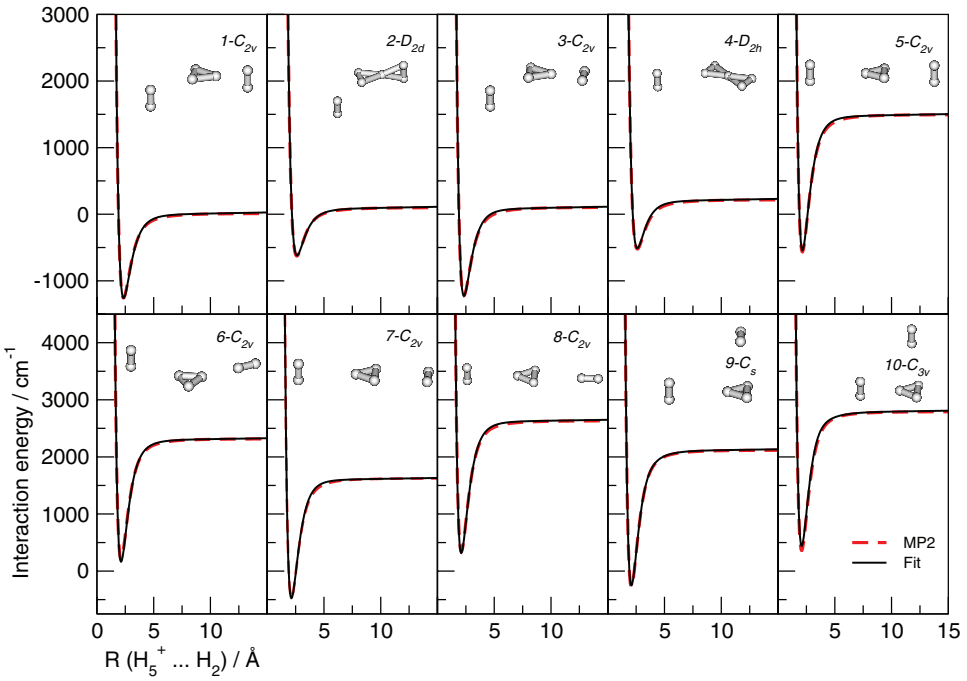

FIG. 5. Interaction energies for the $H_5^+, \ldots, H_2$ as a function of the intermolecular distance R connecting the centers of masses of the H_3^+ core (within the H_5^+), and the other H_2. In the inset we show the corresponding H_5^+ orientation, with the dissociating H_2 at perpendicular orientation with respect to H_3^+ plane.

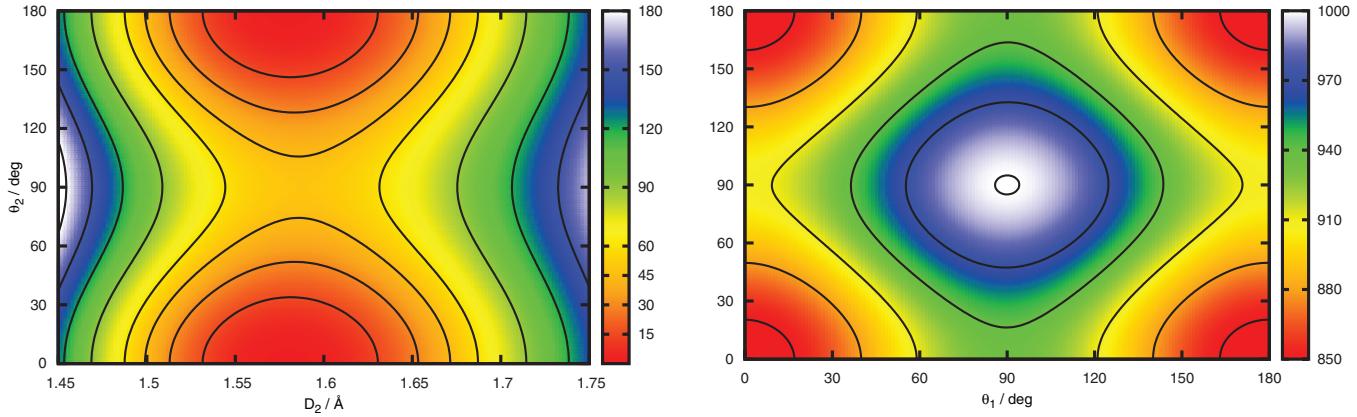

FIG. 6. Contour plots of the H_7^+ potential surface in the (D_2,θ_2)-plane (left panel) with H_7^+ fixed to its 1-C_{2v} orientation, and (θ_1,θ_2)-plane (right panel) with the H_7^+ fixed to its 4-C_{2v} orientation. Contour lines are given in cm^{-1}.

values for perpendicular orientation of the dissociating H_2 molecule. More figures for different orientations of the two fragments are given in the supplementary material.[44] The interaction energies are relative to the $H_5^+ + H_2$ dissociation limit at −3.68222854 a.u. from the MP2 calculation (see Table I). The total energy predicted by the surface at $R = 20$ Å is −3.68221733 a.u., that compares very well with the corresponding MP2 value. By considering this value together with the minimum total energy (see Table IV) a well-depth, D_e, of 1727.9 cm^{-1} is predicted from the present surface, in agreement with the MP2 one, 1725.7 cm^{-1}, given in Table I. As seen in Figure 5, the present potential curves are in excellent agreement with the MP2 *ab initio* data for all the orientations of the H_5^+ and the perpendicular H_2 unit. In general, (see the supplementary material figure) for most of the chosen orientations of the H_5^+ and H_2 fragments we show that the parameterized PES follows very close the MP2 results. Some deviations are only found for high lying configurations, at energies about 2000–3000 cm^{-1} above the dissociation $H_5^+ + H_2$ threshold, corresponding to a 10-C_{3v} orientation of the H_5^+ and for intermolecular distances $R > 5$Å with the H_2 fragment. This should probably be due to the sparsity of *ab initio* energies at those configurations.

For a better overall picture we display in Figures 6 and 7 two-dimensional contour plots of the fitted PES. In Figure 6 we choose projections of the potential values as a function of D_2 and θ_2 (see left panel), and of θ_1 and θ_2 (see right panel). The D_2 coordinate is defined in Figure 1, while θ_1 and θ_2 are the angles between the D_1 and P_1, and D_2 and P_2 ones, respectively. In the left panel, the H_7^+ cluster is fixed at its 1-C_{2v} orientation, and the contour lines of the surface are demonstrated around the two symmetric 1-C_{2v} minima for $D_2 = 1.58$Å and θ_2 at 0 and 180°, respectively, as well as, in the region of the 2-C_s barrier between them at $\theta_2 = 90°$ and 48 cm^{-1} higher in energy than the global minimum. In the right panel, the H_7^+ is kept at the 4-C_{2v} orientation, and we show the details of the surface around its next 4-C_{2v}, 5-C_{2v}, 6-C_{2v}, and 7-C_{2v} stationary points at an energy range of 850–1000 cm^{-1} above the global minimum. The 5-C_{2v} and 6-C_{2v}, both of them second-order saddle points, correspond to the barriers between the two symmetric 4-C_{2v} (first-order saddle) structures, while the 7-C_{2v} (third-order saddle) connects the four symmetric 4-C_{2v} ones.

In Figure 7 the H_7^+ is kept fixed to its 1-C_{2v} orientation, and the projections of the potential surface are shown in the (D_2,$R_1 = R_3$) and (D_2,$P_1 = P_2$) planes in the top and bottom panels, respectively. The region around the 1-C_{2v} potential well together with the dissociation of the H_7^+ to $H_5^+ + H_2$ along the D_2 distance for different isosceles geometries of the H_3^+ core in the H_5^+ fragment up to energies of 30 000 cm^{-1} (see top panel) are shown. The topology of the surface is also provided as a function of the D_2 distance for

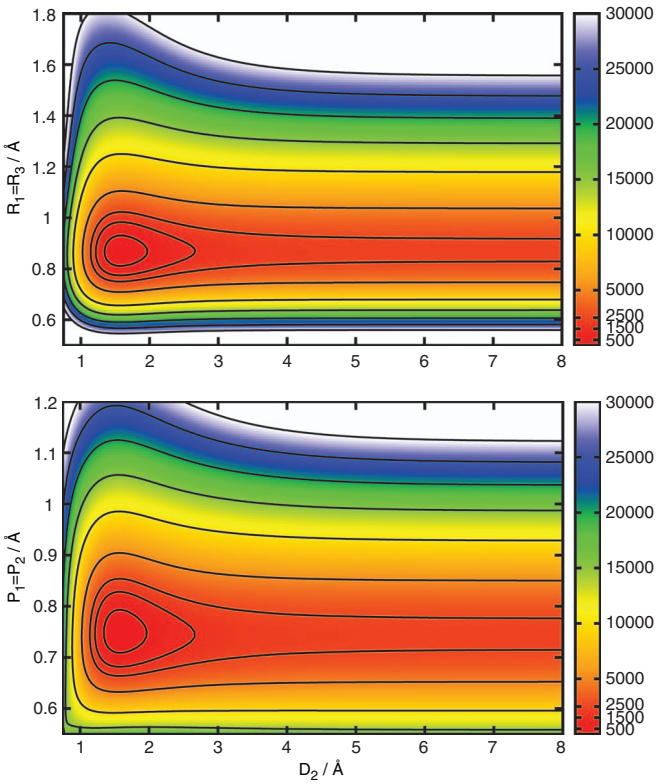

FIG. 7. Contour plots of the H_7^+ potential surface in the (D_2,$R_1 = R_3$) (top panel), and (D_2,$P_1 = P_2$)-plane (bottom panel). The orientation of the H_7^+ is kept at 1-C_{2v}. Contour lines in cm^{-1}.

equal bondlengths of the two H_2 units (see bottom panel). One can see that the PES is flat along the D_2 coordinate, and shows a smooth and correct behavior for the whole configuration space of interest.

As we have already mentioned, up to date there is no analytical PES available in the literature for the H_7^+, and just recently an "on the fly" PES based on DFT calculations has been reported for the H_7^+.[29] The DFT/B3(H) surface has been found to provide a globally correct representation of the H_7^+ PES, however, the quality of the electronic interaction energies is lower compared to the benchmark CCSD(T) results. For the DFT surface an averaged error for the total energies of about 650 cm^{-1} has been reported in comparison with the CCSD(T) data.[29] As we discussed above, the rms error in the fit of the present surface is 170 cm^{-1} with respect the entire set of the MP2 data, that includes the energy difference estimated between the MP2 and CCSD(T) calculations. Thus, the present surface is the most accurate and computationally much more efficient one for the H_7^+ cluster.

IV. SUMMARY AND CONCLUSIONS

We present a full-dimensional, *ab initio* and permutationally invariant surface for the H_7^+. This is the first analytical PES for this 15-dimensional cluster. Taking advantage of computational and methodological progresses made recently in the field, and in particular the capabilities of the invariant polynomial method, was enable to construct an accurate surface for this system. The permutational symmetry with respect to interchange of H atoms is incorporating into the representation of the surface by employing permutationally invariant basis functions in Morse-type variables for all the internuclear distances. The parameterization of the potential is based on *ab initio* MP2 interaction energies of about 160 000 geometries of the system, sampling the configuration space of interest up to energies of 30 000 cm^{-1}.

The topology of the surface is investigated and ten stationary points on the PES are located and characterized by normal-mode analysis. A comparison with benchmark CCSD(T) calculations at these stationary points showed an excellent agreement with an average absolute difference of only 12 cm^{-1}. It was also found that the PES dissociates correctly to the $H_5^+ + H_2$ fragments, with a value for the D_e energy of 1728 cm^{-1} and a rms error up to this energy of 30.5 cm^{-1}. For the entire set of *ab initio* MP2 data the fitted surface has an overall rms error of 170 cm^{-1}. The present fit is the most accurate and computationally efficient representation of the H_7^+ surface, that could motivate further theoretical studies on spectroscopy and dynamics for this cluster.

ACKNOWLEDGMENTS

The authors thank to Centro de Calculo (IFF), Coherent Technologies, Inc. (CTI) (Consejo Superior de Investigaciones Cientificas (CSIC)), and Centro de Supercomputación de Galicia (CESGA) for allocation of computer time. R.P. acknowledges financial support by Ministerio de Ciencia e Innovacion, Spain, Grant No. FIS2010-18132, FIS2011-29596-C02-01 and European Cooperation in Scientific and Technical Research (COST) Action CM1002 (CODECS). P.B. acknowledges a postdoctoral fellowship from the Ramón Areces Foundation, Spain. J.M.B. and Y.W. thank the National Science Foundation (CHE-1145227) for financial support.

[1] M. Isla and J. A. Alonso, J. Chem. Phys. C **111**, 17765 (2007).
[2] J. T. Hallett, D. E. Shemansky, and X. Liu, Astrophys. J. **624**, 448 (2005).
[3] J. Zweiback, R. A. Smith, T. E. Cowan, G. Hays, K. B. Wharton, V. P. Yanovsky, and T. Ditmire, Phys. Rev. Lett. **84**, 2634 (2000).
[4] W.-Q. Deng, X. Xu, and W. A. Goddard, Phys. Rev. Lett. **92**, 166103 (2004).
[5] Y. K. Bae, P. C. Cosby, and D. C. Lorents, Chem. Phys. **159**, 214 (1989).
[6] M. Okumura, L. I. Yeh, and Y. T. Lee, J. Chem. Phys. **83**, 3705 (1985); **88**, 79 (1988).
[7] S. L. Bennett and F. H. Field, J. Am. Chem. Soc. **94**, 8669 (1972).
[8] K. Hiraoka and P. Kebarle, J. Chem. Phys. **62**, 2267 (1975).
[9] R. J. Beuhler, S. Ehrenson, and L. Friedman, J. Chem. Phys. **79**, 5982 (1983).
[10] K. Hiraoka, J. Chem. Phys. **87**, 4048 (1987).
[11] K. Hiraoka and T. Mori, J. Chem. Phys. **91**, 4821 (1989).
[12] E. W. Ignacio and S. Yamabe, Chem. Phys. Lett. **287**, 563 (1998).
[13] M. Barbatti, G. Jalbert, and M. A. C. Nascimento, J. Chem. Phys. **113**, 4230 (2000).
[14] H. Chermette and I. V. Ymmud, Phys. Rev. B **63**, 165427 (2001).
[15] R. Prosmiti, P. Villarreal, and G. Delgado-Barrio, J. Phys. Chem. A **107**, 4768 (2003).
[16] G. E. Moyano and M. A. Collins, J. Chem. Phys. **119**, 5510 (2003).
[17] Z. Xie, B. J. Braams, and J. M. Bowman, J. Chem. Phys. **122**, 224307 (2005).
[18] P. H. Acioli, Z. Xie, B. J. Braams, and J. M. Bowman, J. Chem. Phys. **128**, 104318 (2008).
[19] T. C. Cheng, B. Bandyopadyay, Y. Wang, S. Carter, B. J. Braams, J. M. Bowman, and M. A. Duncan, J. Phys. Chem. Lett. **1**, 758 (2010).
[20] A. Aguado, P. Barragán, R. Prosmiti, G. Delgado-Barrio, P. Villarreal, and O. Roncero, J. Chem. Phys. **133**, 024306 (2010).
[21] P. Barragán, R. Prosmiti, O. Roncero, A. Aguado, P. Villarreal, and G. Delgado-Barrio, J. Chem. Phys. **133**, 054303 (2010).
[22] R. Pérez de Tudela, P. Barragán, R. Prosmiti, P. Villarreal, and G. Delgado-Barrio, J. Phys. Chem. A **115**, 2483 (2011).
[23] P. Barragán, R. Pérez de Tudela, R. Prosmiti, P. Villarreal, and G. Delgado-Barrio, Phys. Scr. **84**, 028109 (2011).
[24] B. A. McGuire, Y. Wang, J. M. Bowman, and S. L. Widicus Weaver, J. Phys. Chem. Lett. **2**, 1405 (2011).
[25] C. Sanz-Sanz, O. Roncero, A. Valdés, R. Prosmiti, G. Delgado-Barrio, P. Villarreal, P. Barragán, and A. Aguado, Phys. Rev. A **84**, 060502 (2011); A. Valdés, P. Barragán, C. Sanz-Sanz, R. Prosmiti, P. Villarreal, and G. Delgado-Barrio, Theor. Chem. Acc. **131**, 1210 (2012).
[26] A. Valdés, R. Prosmiti, and G. Delgado-Barrio, J. Chem. Phys. **136**, 104302 (2012).
[27] I. Štich, D. Marx, M. Parrinello, and K. Terakura, J. Chem. Phys. **107**, 9482 (1997).
[28] Y. Ohta, J. Ohta, and K. Kinugawa, J. Chem. Phys. **121**, 10991 (2004).
[29] P. Barragán and R. Prosmiti, Int. J. Quantum Chem. (2012).
[30] H. Chermette, H. Razafinjanahary, and L. Carrion, J. Chem. Phys. **107**, 10643 (1997).
[31] P. Barragán, R. Prosmiti, P. Villarreal, and G. Delgado-Barrio, Int. J. Quantum Chem. **111**, 368 (2011).
[32] L. M. Raff, M. Malshe, M. Hagan, D. I. Doughan, M. G. Rockley, and R. Komanduri, J. Chem. Phys. **122**, 084104 (2005).
[33] R. Dawes, D. L. Thompson, Y. Guo, A. F. Wagner, and M. Minkoff, J. Chem. Phys. **126**, 184108 (2007).
[34] J. Behler and M. Parrinello, Phys. Rev. Lett. **98**, 146401 (2007).
[35] S. Manzhos and T. Carrington, Jr., J. Chem. Phys. **129**, 224104 (2008).
[36] B. J. Braams and J. M. Bowman, Int. Rev. Phys. Chem. **28**, 577 (2009).
[37] X. Huang, B. J. Braams, and J. M. Bowman, J. Chem. Phys. **122**, 044308 (2005).

[38]J. Zin, B. J. Braams, and J. M. Bowman, J. Phys. Chem. A **110**, 1569 (2006).
[39]Y. Wang, X. Huang, B. C. Shepler, B. J. Braams, and J. M. Bowman, J. Chem. Phys. **134**, 094509 (2011).
[40]H.-J. Werner, P. J. Knowles, R. Lindh, F. R. Manby, M. Schütz *et al.*, MOLPRO, version 2009.1, a package of *ab initio* programs, 2009, see http://www.molpro.net.
[41]H. Derksen and G. Kemper, *Computational Invariant Theory* (Springer-Verlag, Berlin, 2002).
[42]W. Bosma, J. Cannon, and C. Playoust, J. Symb. Comput. **24**, 255 (1997); See http://magma.maths.usyd.edu.au/magma/ for information about MAGMA computational algebra software package.
[43]R. Prosmiti, A. A. Buchachenko, P. Villarreal, and G. Delgado-Barrio, Theor. Chem. Acc. **106**, 426 (2001).
[44]See supplementary material at http://dx.doi.org/10.1063/1.4726126 for the harmonic frequencies of the ten stationary points of the PES, and additional figures with the potential values for different orientations of the H_7^+.